On the link between Beamforming and Kernel-based Source Inversion

Daniel Bowden[1]*, Korbinian Sager[1 2], Andreas Fichtner[1], Małgorzata Joanna Chmiel[1]: 1. ETH Zürich, 2. Brown University, *daniel.bowden@erdw.ethz.ch

1. Introduction

Beamforming and backprojection methods offer a data-driven approach to image noise sources, but provide no opportunity to account for prior information or iterate through an inversion framework. In contrast, recent methods have been developed to locate ambient noise sources based on cross-correlations between stations and the construction of finite-frequency kernels, allowing for inversions over multiple iterations (i.e., Tromp et al., 2010, Ermert et al. 2017, Sager et al. 2018). These kernel-based approaches show great promise, both in mathematical rigour and in results, but may remain difficult to understand or implement for the wider community. Here we show that these two different classes of methods, beamforming and kernel-based inversion, are achieving exactly the same result in certain circumstances. This means existing beamforming and backprojection methods can also incorporate prior information in a mathematically correct manner.

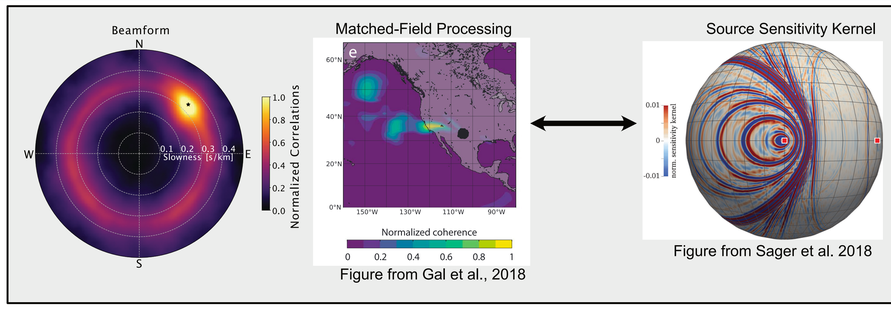

Figure from Gal et al., 2018

Figure from Sager et al. 2018

Conclusion & Takeaways:

Beamforming / Backprojection and Full Waveform Source Inversion are similar*

*at least for the first iteration, depending on starting model, disregarding windowing choices, other restrictions apply

Both communities can learn from each other:

1) Beamform/backprojection methods should be more rigorous; can account for prior information

2) Full-waveform modelers can adapt the processing tricks developed by the beamform/ backprojection community

Beamforming

We start with a straightforward correlation-based beamformer:

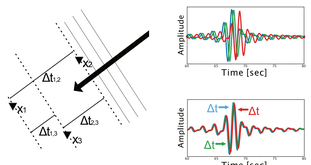

Grid search over azimuths and slownesses. Each slowness defines a plane wave, for which delay times are calculated.

Time shifts are applied.

Zero-lag correlation coefficients give a "score."

Sum over station pairs.

$$C_{ij}(s_x, s_y) = \int_{-T}^{T} u_z(\boldsymbol{x}_i, t - \Delta t_{ij}(s_x, s_y)) u_z(\boldsymbol{x}_j, t) dt$$

$$P(s_x, s_y) = \sum_{i,j} C_{ij}(s_x, s_y)$$

A synthetic 2D example. Noise sources are a homogenous background, with a stronger source to the North-East.

Synthetics are modelled with the Generalised Interferometry scripts of Fichtner et al., 2016

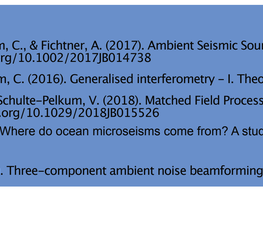

Backprojection

Here specifically **Matched Field Processing**, is the same shifting-and-correlating process, just with a gridsearch over some spatial domain instead of over azimuths.

In this case we use only two-stations, and only one source marked with a star.

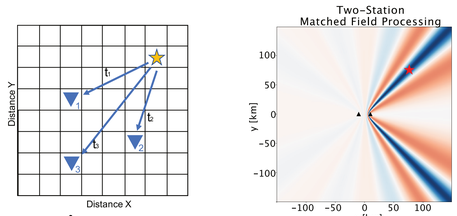

Gridsearch over (x,y) locations here, apply time shifts and correlate to create this figure.

Change the order

Instead of applying time shifts separately, collect cross correlations first.

The time shift (whether in slowness-domain or a spatial-domain) just tells you where in the cross correlation to look.

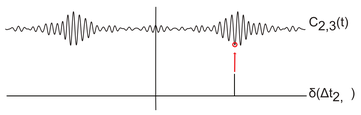

$$C_{ij}(t) = \int_{-T}^{T} u_z(\boldsymbol{x}_i, \tau)\, u_z(\boldsymbol{x}_j, \tau + t)\, d\tau$$

$$P(s_x, s_y) = \sum_{i,j} \int_{-T}^{T} \delta(\Delta t_{ij}(s_x, s_y))\, C_{ij}(t)\, dt$$

Instead of a delta function, we might use some window of finite length. This could, for example, represent prior expectations of wavelength-imposed smoothing on the final image.

$$P(s_x, s_y) = \sum_{i,j} \int_{-T}^{T} W_{ij}(t, s_x, s_y)\, C_{ij}(t)\, dt$$

Add Prior Information

Now it gets fun.

With some knowledge of the background noise field, we can compute synthetic waveforms and compare. The equation below uses a least-squares misfit, but others are possible.

$$\sum_{i,j} \int_{-T}^{T} \Big[W_{ij}(t, s_x, s_y)\, C_{ij}^{obs}(t) - W_{ij}(t, s_x, s_y)\, C_{ij}^{syn}(t) \Big]^2 dt = \mathcal{X}(s_x, s_y)$$

Data Model Misfit

Iterate

The misfit describes the discrepancy between data and model. We could now gridsearch again, perturbing the model gridpoints one-by-one and testing how this affects that misfit. This gives us a gradient, which guides updates to the model. The following shows a first gradient computed for a homogeneous starting model.

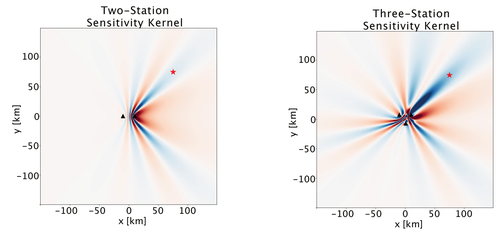

A Note on Efficiency:

Nowhere else on this display do we mention adjoint methods. This is on purpose.
Everything described up until now could be described by gridsearching and perturbing a model. However, that would be computationally terribly inefficient. Fortunately, there are tricks, like directly computing the **noise correlation wavefield** and using **adjoint methods** to get a gradient appropriate to a particular misfit.

These are not described here, but see our paper coming soon!

A win-win situation:

Better beamforms

We can take what we've learned back to beamforming. This is how our misfit function looks for nearly all existing beamform algorithms:

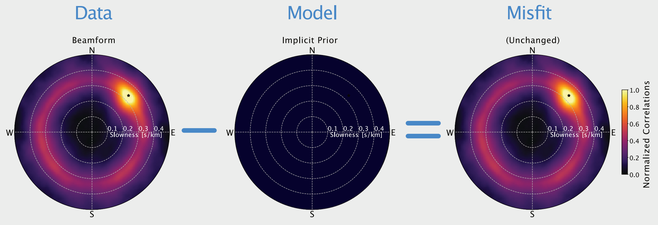

If instead we assume a homogeneous distribution of background sources as our prior model, we can easily see if something else remains. This is similar to deconvolving an array response function, but accounting for **both** array geometry and source assumptions.

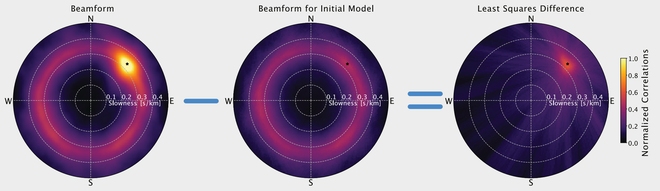

Even though we (the ambient noise community) love to assume we have a homogeneous background distribution of noise sources, we never implement this when it comes to beamforming. The **implicit** uniform prior used in the first row states that energy is equally likely to be propagating across the array at all slownesses, or that there is simply no energy whatsoever. Both of those statements are actually very strong and unrealistic.

Better pre-processing

If one has cross-correlated data for interferometry, creating a beamform representatin of those correlations is trivial (see "Change the Order" above). If we use various preprocessing techniques to get better noise correlation functions, we can directly see the effect that has on our **effective** noise source distribution.

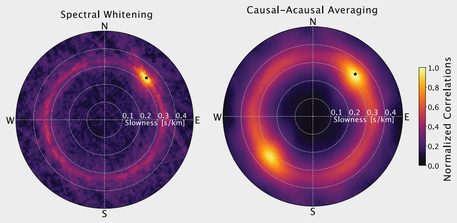

See also Fichtner et al., 2016, for kernel-based images of the effect of preprocessing. Also, see Seydoux et al., 2017 for an approach that exploits beamforms to "even out" the incident wavefield for better correlation function convergence.

Better Source Inversions

1) The beamforming/backprojection community has numerous image enhancement tools which could be incorporated into inversion frameworks, such as:

– Using 3-component beamformers to constrain wavetype and polarization: Löer et al. 2018, Juretzek and Hadziioannou 2016, Gal et al. 2018. This is already used for inversions by Xu et al., 2019!

– Using eigenvalue decompositions or other math tricks to isolate unique signals (i.e., MUSIC, MDVR, etc.)

2) Furthermore, Inversion schemes often rely on defining direct surface-wave windows (or other phases) to compute misfits on. This is an unnecessary restriction. Instead, something like a beamform map can directly inform where in a correlation to look. Also informative: a record section, slant stack, vespa-diagram, etc. (Retailleau et al. 2017).

For a source to the North East, Station Pair 1 will have stronger energy in the surface wave window. Station Pair 2 also has energy, but we miss it.

The beamform map is degraded.

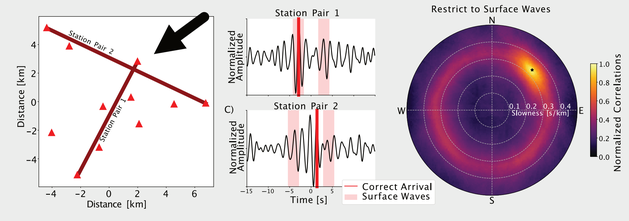

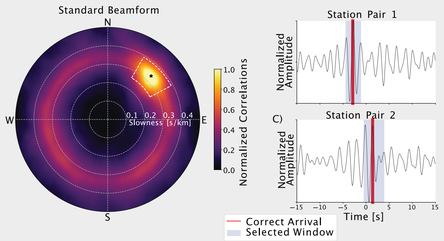

Targeting where to look in advance will better capture relevant information.

These blue windows would be better suited for an inversion scheme to image this source.

References:

Ermert, L., Sager, K., Afanasiev, M., Boehm, C., & Fichtner, A. (2017). Ambient Seismic Source Inversion in a Heterogeneous Earth: Theory and Application to the Earth's Hum. Journal of Geophysical Research: Solid Earth, 122(11), 9184–9207. https://doi.org/10.1002/2017JB014738

Fichtner, A., Stehly, L., Ermert, L., & Boehm, C. (2016). Generalised interferometry – I. Theory for inter-station correlations. Geophysical Journal International, ggw420. https://doi.org/10.1093/gji/ggw420

Gal, M., Reading, A. M., Rawlinson, N., & Schulte-Pelkum, V. (2018). Matched Field Processing of Three-Component Seismic Array Data Applied to Rayleigh and Love Microseisms. Journal of Geophysical Research: Solid Earth, 123, 6871–6889. https://doi.org/10.1029/2018JB015526

Juretzek, C., & Hadziioannou, C. (2016). Where do ocean microseisms come from? A study of Love-to-Rayleigh wave ratios. Journal of Geophysical Research: Solid Earth, 121(9), 6741–6756. https://doi.org/10.1002/2016JB013017

Löer, K., Riahi, N., & Saenger, E. H. (2018). Three-component ambient noise beamforming in the Parkfield area. Geophysical Journal International, 1478–1491. https://doi.org/10.1093/gji/ggy058

Retailleau, L., Boué, P., Stehly, L., & Campillo, M. (2017). Locating Microseism Sources Using Spurious Arrivals in Intercontinental Noise Correlations. Journal of Geophysical Research: Solid Earth, 122(10), 8107–8120. https://doi.org/10.1002/2017JB014593

Sager, K., Ermert, L., Boehm, C., & Fichtner, A. (2018). Towards full waveform ambient noise inversion. Geophysical Journal International, 212(1), 566–590. https://doi.org/10.1093/gji/ggx429

Seydoux, L., de Rosny, J., & Shapiro, N. M. (2017). Pre-processing ambient noise cross-correlations with equalizing the covariance matrix eigenspectrum. Geophysical Journal International, 210(3), 1432–1449. https://doi.org/10.1093/gji/ggx250

Tromp, J., Luo, Y., Hanasoge, S., & Peter, D. (2010). Noise cross-correlation sensitivity kernels. Geophysical Journal International, 183(2), 791–819. https://doi.org/10.1111/j.1365-246X.2010.04721.x

Xu, Z., Mikesell, T. D., & Gribler, G. (2019). Rayleigh-wave multicomponent crosscorrelation-based source strength distribution inversion. Part 1 : Theory and numerical examples. Geophysical Journal International, 218(3), 1761–1780. https://doi.org/10.1093/gji/ggz261 [especially see Appendix C!]